MICROWAVE ASSISTED SOL-GEL SYNTHESIZED MAGNETITE (FE_3O_4) NANOPARTICLES FOR CONTINUOUS FLOW ADSORPTIVE REMOVAL OF COPPER (II) IONS

Pramod M. Agale[1], Satish P. Meshram[2], Shrikant S. Barkade[3]
[1]Dept. of Chemistry, Guhagar Education Society's, KDB College, Guhagar (Maharashtra)
[2]Centre for materials for electronics technology (C-MET), Panchwati off Pashan, Pune (Maharashtra)
[3]Department of Chemical Engineering, Sinhgad College of Engineering, Pune (Maharashtra)

Abstract

Herein this article, we are reporting facile microwave assisted sol-gel method for synthesis of magnetite (Fe3O4) nanoparticles. These as-synthesized nanoparticles were further used for adsorptive removal of Cu (II) ions from aqueous solution. Magnetite (Fe3O4) nanoparticles were characterized in terms of chemical composition, phase, structure, morphology and particle size using variety of characterization techniques viz. Fourier transform infrared spectroscopy (FTIR), X-ray diffraction (XRD) and Transmission electron microscopy (TEM). FTIR analysis confirmed presence of Fe-O and XRD results revealed cubic spinel structure of magnetite nanoparticles. TEM analysis revealed particle size about 20-60 nm. Column studies were performed to evaluate effects of various parameters such as pH, initial copper ion concentration and flow rate on Cu (II) adsorption. Further, model parameters were evaluated for Yoon-Nelson, Thomas and Adams-Bohart model by linear regression analysis for Cu (II) adsorption results. The obtained experimental data was found to best fitted with Yoon-Nelson and Thomas model compared to Adams-Bohart model.

Key words: Magnetite, Microwave assisted sol-gel, Cu (II) adsorption, Column study, Adsorption kinetic models

I. INTRODUCTION

Industrial wastewater contains higher amount of heavy metals that can pollute the water when discharged into it [1]. Toxic heavy metals of particular concern in industrial wastewaters include zinc, copper, nickel, mercury, cadmium, lead, arsenic and chromium. At least 20 metals are considered to be toxic and approximately half of these metals are emitted in to the environment in quantities that are risky to the surroundings as well as human health [2]. Copper is an essential trace element that is vital to the health of all living things but excess exposure or presence adversely affects all living things. It targets organs like liver, bone, nervous system and immune systems. Also, too much copper can cause vomiting, diarrhea, stomach cramps, and nausea. It also causes liver damage and kidney disease. Ingestion of 15-75 mg of copper can cause gastro-intestinal disorder. Copper toxicity can cause irritation, corrosion, hepatic damage and central nervous system irritation followed by depression. Prescribed limit for copper in drinking water is 0.05 mg/L as per WHO norms and also 0.05 mg/L as per ISI prescribed limits [3]. Different treatment processes that have been used to remove heavy metals from wastewater include precipitation, coagulation, ion exchange, electro-dialysis, membrane filtration, flotation, and reverse osmosis [4-6]. However, they have their own limitations such as high cost and low efficiency of removing trace level of heavy metal

ions compared to adsorption method.

Adsorption is used in many industries for water purification due to its low cost and applicability on large scale [7]. Some researchers investigated the adsorbents which could be used for water treatment with higher output and lower costs, but have a very little regeneration capabilities for recovering purposes. High regeneration cost would lead to an uneconomical recovery of adsorbents, and consequently the resultant wastes would cause a secondary pollution to the environment [8]. Therefore, it is necessary to explore a new effective adsorbent with large surface area, as well as low regeneration cost. For water purification, there is a need of technologies that have ability to remove toxic contaminants from the environment, rapidly, efficiently, and within a reasonable cost. Thus, development of novel nanomaterials with increased affinity, capacity and selectivity for heavy metals is an active emerging area of research [9].

Nanoadsorbents are nanoscale particles or nanocomposites of organic/inorganic materials that have high affinity to adsorb substances due to small size and high surface area. Nanosorbents can be designed to have multiple reactive nanoparticles or nanostructure components to target specific contaminants and offer the opportunity of even greater sorption capacities. Hence it is significantly improved remediation technology in terms of efficiency, selectivity and specificity when compared to conventional technologies [10]. Among the various kinds of nanoadsorbents, oxide based nanomaterials such as Fe_3O_4, TiO_2, ZnO and their composites play an important role. Recently, there have been several reports on magnetic oxides, especially Fe_3O_4 being used as nanoadsorbents for the removal of various toxic heavy metal ions from wastewater, such as Ni^{2+}, Cu^{2+}, Cd^{2+}, Hg^{2+},Pb^{2+}, Zn^{2+}, Co^{2+}, Cr^{3+} and As^{3+} [11]. Magnetite nanoparticles have one more special property in the form of supermagnetism along with small size and high surface area. Currently iron oxide nanoparticles with novel properties and functions are being widely studied in the field of separation due to its cost effective synthesis, easy coating and surface modification [12]. Also their ability to control or manipulate materials on a nanoscale dimensions provide amazing versatility in separation techniques [13]. Apart from these, low toxicity, chemical inertness and biocompatibility makes it a good adsorbent for heavy metal removal. Also they can be reused after magnetic separation for removing the adsorbed toxic contaminants. Moreover, their surface modification by the attachment of inorganic shells and organic molecules stabilizes and prevents oxidation of nanoparticles [14]. These surface functionalities provide sites for the uptake of specific/selective metal ions and, thus, enhance the efficiency of the removal process [15]. In this scenerio, Afnidar *et al.* reported removal of Cd (II) ions using magnetite nanocomposite in fixed bed [16]. Yuan *et al.* reported two step sol-gel approach followed by ultrasonication for synthesizing amino-functionalized SiO_2-meso-SiO_2-R_2-NH_1 with particles sized 2.1 nm, effectively removing Cu (II), Cd (II) and Pb (II) [17]. Wang *et al.* developed amino-functionalized Fe_3O_4-SiO_2 magnetic nanomaterial to remove Cu (II), Cd (II), and Pb (II) from aqueous media [18]. Liu *et al.*via co-precipitation method synthesized humic acid functionalized Fe_3O_4 nanoparticles for removing Cu (II), Pb (II), Cd (II) and Hg (II) ions [19]. Xin *et al.* synthesized amine-functionalized mesoporous Fe_3O_4 nanoparticles for highly efficient removal of toxic heavy metal ions such as Cu (II), Pb (II) and Cd (II) from water. Removal efficiency is around 98% [20]. Reza *et al.* functionalized salicylic acid on silica-coated magnetite nanoparticles to remove Cu (II), Cd (II), Ni (II) and Cr (III) ions [21]. Faraji *et al.* reported sodium dodecyl sulphate coated Fe_3O_4 nanoparticles (SDS-Fe_3O_4NPs) to remove Cu (II), Ni (II) and Zn (II) ions from water and wastewater samples [22]. Kim *et al.* via hydrothermal route synthesized Fe_3O_4-MnO_2 nanocomposite, effectively removing Cu (II), Cd (II), Pb (II) and Zn (II) ions [23]. Zhang *et al.* developed Fe_3O_4-SiO_2-poly(1, 2-diaminobenzene) nanoparticles for the removal of Cu (II), As (III) and Cr (III) ions from aqueous solution. Particles had core shell structure with particle size ranging from 23-27nm [24]. Xiao *et al.* prepared carboxylated multi-wall carbon nanotube (c-MWCNT)-Fe_3O_4 magnetic hybrids for removing Cu (II) ions [25]. Xin *et al.* reports a simple and efficient chemical method to

decorate multi-walled carbon nanotubes (MWCNTs) with iron oxide (Fe_3O_4) nanoparticles. The size of the nanoparticles ranges from 30 to 50 nm, effectively removing Cu (II) ions [26]. Banerjee *et al*. developed nano-adsorbent by treating Fe_3O_4 nanoparticles with gum arabic to remove copper ions from aqueous solutions. Particle size was found to be 13-67 nm having spinel morphology which effectively removed Cu ions [27]. Chang *et al*. synthesized chitosan-bound Fe_3O_4 nanoparticles via carbodiimide activation forming 13.5 nm particles effectively removing Cu (II) with maximum adsorption capacity of 21.5 mg/g [28]. Badruddoza *et al.* successfully grafted CM-β-CD on the surface of Fe_3O_4 nanoparticles forming ellipsoidal magnetic nanoparticles with 12 nm size to remove Cu (II) ions [29]. There are several methods for the synthesis of nano-sized iron oxide particles, including laser vaporization, hydrothermal synthesis, solvothermal, sol-gel, combustion aerosol synthesis, etc [30].

Among them, sol-gel method has recently been attracting much attention since it provides a simple, economic and effective method to produce high quality particles. The key feature of sol-gel method is that it provides the opportunity to control structure of final particles at the beginning of the process itself [31]. Microwave assisted method is another significant alternative that has gained attention in recent years as a simple, rapid and efficient process for growth of nanostructured oxides. In microwave heating electromagnetic radiations are converted into dipolar rotation and ionic conduction, which in turn are related to chemistry of reaction mixture. Thus selective heating of compounds in reaction mixture can be achieved, as different compounds have different microwave absorbing properties. The general advantages of microwave mediated synthesis over conventional ones are reaction rate acceleration as a consequence of high heating rates, wide range of reaction conditions, that is, mild conditions or autoclave conditions, high reaction yields, reaction selectivity due to different microwave absorbing properties, excellent control over reaction conditions, and simple handling, allowing simple and fast optimization of experimental parameters [32].

The application of the microwave technique to iron oxide nanoparticles fabrication is due, and, in fact, several microwave-assisted synthesis of iron oxide nanoparticles for heavy metal ions removal have been reported; however, in these preliminary cases, the protocols have either required toxic additives, or the nanoparticles that were produced lacked monodispersity [33], or required a phase transfer step to confer water solubility [34]. The objective of this study is to synthesize, characterize magnetite nanoparticles by microwave assisted sol-gel method and investigate its application in Cu (II) ion removal.

II. EXPERIMENTAL

A. *Regents and standard solutions*

Materials used in this work were of analytical grades and include Ferric nitrate ($Fe(NO_3)_3.9H_2O$), ethylene glycol ($C_2H_6O_2$), copper sulfate pentahydrate ($CuSO_4.5\ H_2O$), ammonia and nitric acid. Distilled water was used throughout this work. Stock solutions of copper ions were prepared by dissolving $CuSO_4$ in distilled water.

B. *Preparation of Fe_3O_4 nanoparticles*

In a typical synthesis process of Fe_3O_4 nanoparticles, 5 gm of ferric nitrate was added to 10 mL ethylene glycol and was stirred for 2 hours at 40^{o}C at 600 rpm. Then the prepared sol was placed in microwave oven (LG MS2021CW, 2.45GHz) and was heated using microwave radiation power of 350 W for 20 min. After few minutes of irradiation, gel is formed and it breaks down again to liquid. The obtained sample was filtered using whatman filter and then was dried at 150 ^{o}C in oven. The sample was then mortared and calcinied at 300 ^{o}C in muffle furnace yielding magnetite nanoparticles [35]. The overall experimental set-up is as shown in Figure 1.

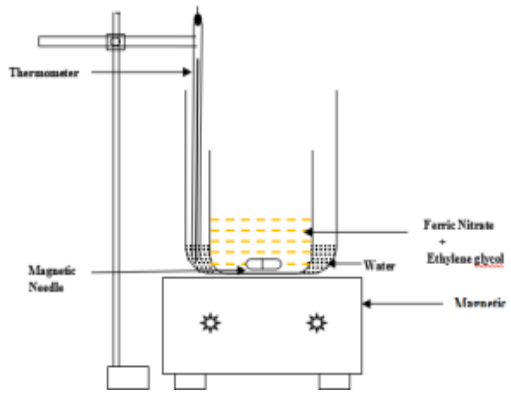

Fig. 1. Assembly for synthesis of magnetite nanoparticles using sol-gel method

C. Characterization techniques

Infrared spectra of the samples were obtained using a FTIR spectrophotometer (Perkin Elmer/Spectrum EXII) in KBr pellets. The phases were identified by the means of X-ray diffraction (Bruker D8 advance diffractometer with Cu K-α radiation). The size and morphology were observed by Transmission electron microscope (Philips CM200).

D. Column adsorption studies for removal of Cu (II) ions

Stock solution of Cu (II) ions was prepared in distilled water and was used for column adsorption studies. Adsorption in a continuous flow system was done in a fixed bed column (i.d. = 130 mm and length = 700 mm). Bed of adsorbent of fixed height was used with glass wool placed at the bottom. The addition of glass wool was made to improve the flow distribution. Aqueous Cu (II) ion solution was pumped through column at a desired flow rate by a peristaltic pump (Electrolab PP 50V) in an up flow mode. Samples were collected from the exit of the column and analyzed for copper using UV spectrophotometer (Systronics UV-106). During study various parameters viz. effect of pH, effect of initial Cu (II) ion concentration, and effect of flow rate were screened.

- Effect of pH

The effect of varying pH (3-7) on adsorption of Cu (II) ions is studied. The flow rate of 1.0 mL/min and initial Cu (II) ion concentration of 600 mg/L was maintained.

- Effect of initial Cu (II) ion concentration

Different initial Cu (II) ion concentrations (150-550 mg/L) were used and the effect on the column performance was analyzed. The pH was maintained at 6 and flow rate at 1.0 mL/min, respectively.

- Effect of flow rate

Different flow rates (1-3 mL/min) were used and the effect on the column performance was analyzed. The initial inlet concentration was maintained at 550 mg/L at pH6 respectively.

III. Result and Discussion

A. Synthesis of Fe_3O_4 nanoparticles

In the microwave-assisted sol-gel synthesis of magnetic nanoparticles, the unpaired electron (Fe^{3+}) present in sol are excited to higher energy state due to absorption of microwaves. Coupling between magnetic and microwaves field converts radiation energy to heat. Thus in few minutes due to conversion of radiation waves to heat, gel is formed and it breaks down again to liquid. This is then filtered, dried and mortared to obtain magnetite nanoparticles.

B. Characterization of as-synthesized Fe_3O_4 nanoparticles

FTIR spectrum was recorded as a function of transmission and wavelength in the range of 400-4000 cm^{-1}. Figure 2 shows the FTIR spectrum of as-synthesized Fe3O4 nanoparticles. In spectrum, the absorption peak observed at 553.23 cm^{-1} can be attributed to Fe-O bond. The absorption peak 1070.91 cm^{-1}arises due to strong C-O stretching. The peaks in range of 2916.15 $cm^{-1}$and 2355.77 cm^{-1} can be allocated to tensional vibrations of hydroxyl groups [36].

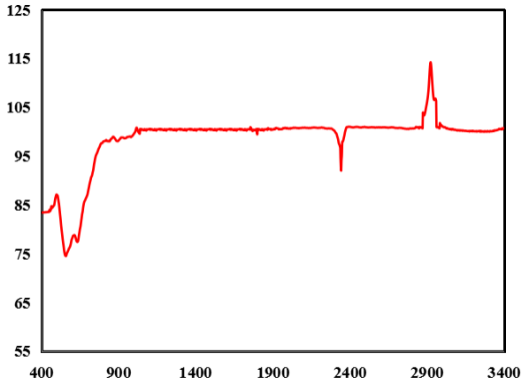

Fig. 2. FTIR spectra for magnetite nanoparticles

Fig. 3 depicts the XRD pattern of microwave assisted sol-gel synthesized magnetite nanoparticles. The main diffraction peaks at θ = 29°, 35° and 42° can be assigned to (2 2 0), (3 1 1) and (4 0 0) phases of cubic spinel structured magnetite crystals (JCPDS 79-0418). No other peak related to other phases of iron oxide nanoparticles is seen. Usually it is not easy to distinguish between γ-Fe_2O_3 from Fe_3O_4 because of similar structure. Also Fe_3O_4 nanoparticles are quite sensitive to oxygen even at low temperature resulting in oxidation of surface of Fe_3O_4 to γ-Fe_2O_3 during drying. Oxidation of Fe_3O_4 to γ-Fe_2O_3 indicates that spinel structure was maintained during this process only valence alteration of iron ions takes place. Thus microwave heating results in high reaction temperatures, faster nucleation, less reaction time, and yielding more crystalline particles [37, 38].

TEM image of as-synthesized Fe_3O_4 nanoparticles is shown in Figure 4. From figure it revealed that the synthesized magnetite nanoparticles are having spherical morphology and are in the range of 20-60 nm.

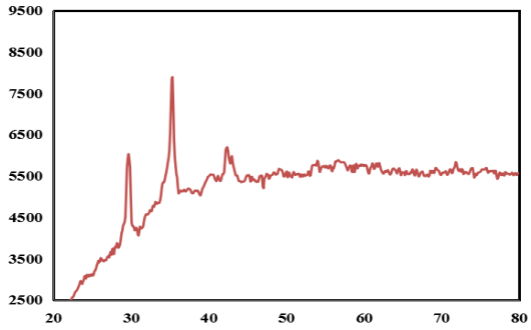

Fig. 3. XRD pattern for magnetite nanoparticles

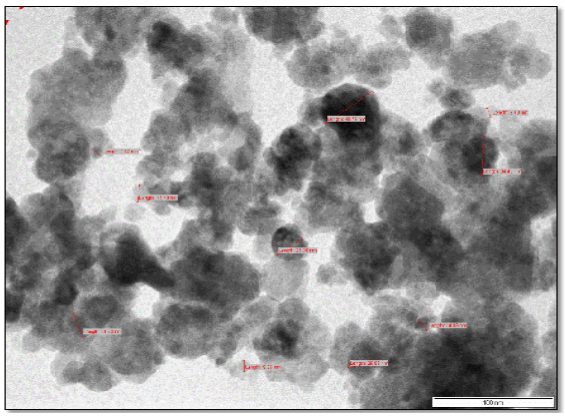

Fig. 4. TEM micrograph of microwave assisted sol-gel synthesized magnetite nanoparticles

C. Cu (II) ion Continuous flow adsorption studies

The as-synthesized magnetite nanoparticles were further evaluated for adsorptive removal of Cu (II) ions in continuous flow using column. The following section discusses the effect of different operating paprameters.

Effect of pH

The capacity of an adsorbent for adsorption of heavy metal ions depends on its chemical and physical properties, target metal ions, hydrolysis capacity of the metal ions and the competitive adsorption of coexisting matters in aqueous solution. The effect of varying pH (3 - 7) on adsorption of Cu (II) ions, with initial Cu (II) ions concentration of 600 mg/L and flow rate of 1.0 mL/min is as shown in Figure 5. Results reveals that as pH increases adsorption increases, since metal ions (i.e. cation) have tendency to hydrate in aqueous solution with increase in pH value. At lower pH values, presence of H^+ ions results in repulsive forces between H^+ and copper ions resulting in lesser adsorption. Also as the solution passes through the column, adsorbent becomes protonated i.e., surface becomes positively charged thus resulting in lesser adsorption. However with increase in pH from 5-6, due to presence of OH^- ions adsorption increases. But at higher pH, light blue colored precipitate is formed and the entire copper ions settles down so adsorption experiments were performed at pH = 6.

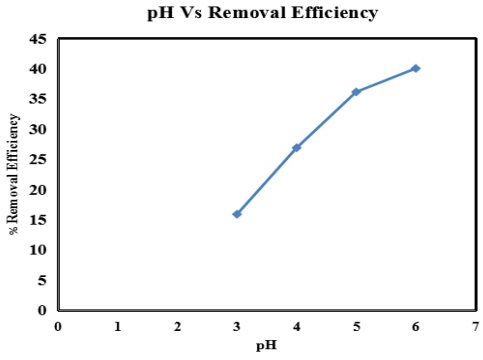

Fig. 5. Effect of pH on removal of Cu (II) ions

Effect of initial Cu concentration

Different initial Cu (II) ions concentrations ranging from 150-550 mg/L were used and the effect on the column adsorption performance was analyzed. The pH and flow rate were maintained at 6 and 1.0 mL/min, respectively. With increase in Cu (II) ion concentrations, adsorption increases thus resulting in increase in efficiency as seen in Figure 6. However, further increase in concentrations, results in lesser adsorption due to limited active sites.

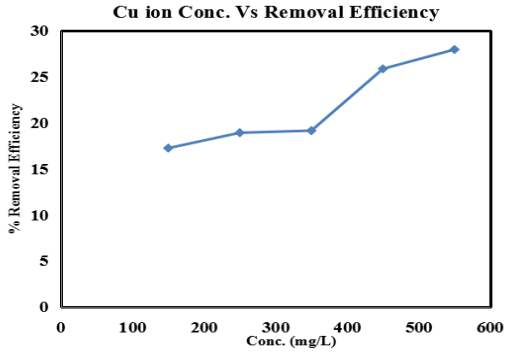

Fig. 6. Effect of initial Cu ion concentration on removal of Cu (II) ions

Effect of flow rate

Different flow rates (1-3 mL/min) were used and the effect on column performance was analyzed. The initial Cu ions concentration and pH were maintained at 550 mg/L and 6, respectively. As seen in Figure 7, lower flow rate results in higher copper ions removal. At low flow rate, the residence of adsorbate was more and hence adsorbent got more time for adsorption of Cu ions as compared to higher flow rates thus resulting in higher adsorption. Thus, efficiency decreases with increase in flow rate. Further increase in flow rate results in carryover of adsorbent.

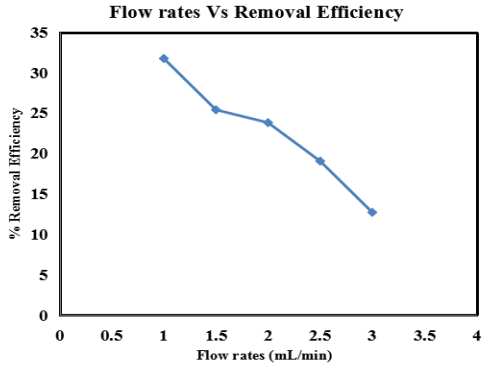

Fig. 7. Effect of flow rates on removal of Cu (II) ions

Model

Yoon-Nelson, Thomas and Adams-Bohart kinetic models were used to analyze the column performance.

Yoon-Nelson Model

Yoon and Nelson developed a model [39] based on the assumption that the rate of decrease in the probability of adsorption is proportional to the probability of adsorbate adsorption and adsorbate breakthrough on the adsorbent. Yoon-Nelson model can be expressed as follows

$$\ln\frac{C_t}{C_0 - C_t} = k_{YN}t - \tau k_{YN}$$

Where k_{YN} (L/min) is the rate velocity constant, τ (min) is the time required for 50% adsorbate breakthrough. A linear plot of ln [C_t/(C_0-C_t)] against sampling time (t) determines the values of τ and k_{YN} from the intercept and slope of the plot (Fig. 8a-8c).

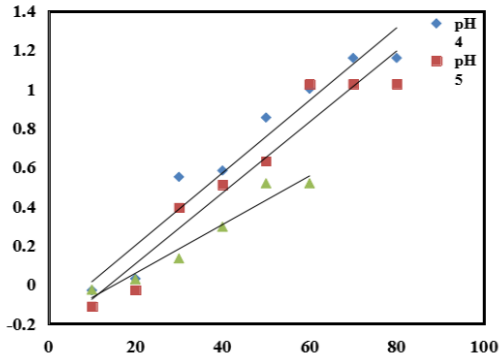

Fig. 8a. Linear Plot of Yoon-Nelson model with experimental data at different pH, C_0= 600 mg/L, Q_0= 1 mL/min

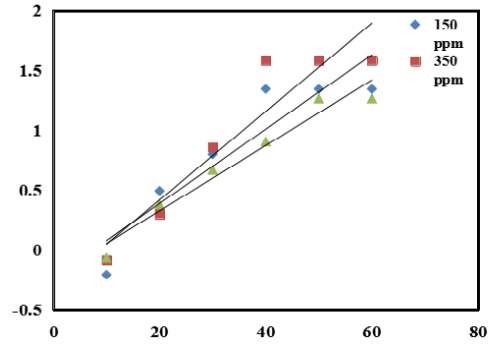

Fig. 8b. Linear Plot of Yoon-Nelson model with experimental data at different concentrations, pH=6, Q_0= 1 mL/min.

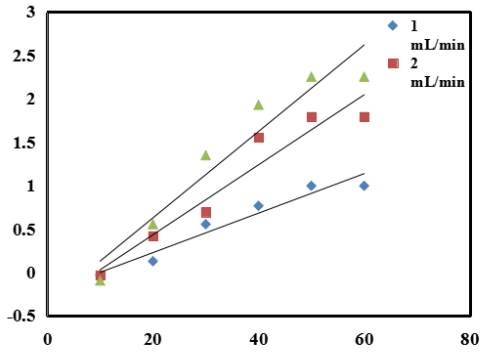

Fig. 8c. Linear Plot of Yoon-Nelson model with experimental data at different flow rate, C_0= 550 mg/L, pH= 6

Table 1
Yoon-Nelson model parameters for Cu (II) adsorption at various operating conditions

pH	Q_0 (mL/ min)	C_0 (mg/ L)	τ (min s)	k_{YN} (min^{-1})	R^2
4	1	600	9.5	0.018 6	0.937
5	1	600	14.27	0.018 1	0.933
6	1	600	15.91	0.012	0.950
6	1	150	11.07	0.039	0.924
6	1	350	10.22	0.044	0.947
6	1	550	8.148	0.027	0.955
6	1	550	10.31	0.022	0.942
6	2	550	9.325	0.040	0.931
6	3	550	7.51	0.049	0.925

Values of τ and k_{YN} are listed in Table 1. Values of R^2 were between 0.92 and 0.95. From Table 1, the rate constant k_{YN} decreases and the 50% breakthrough time τ increases with increasing pH. Also with increase in Cu ion concentration, τ decreases. With increasing flow rate, the values of τ decreases because of less residence time of copper ions in adsorbent bed, while the values of k_{YN} increases.

Thomas Model

Thomas model [40] can be expressed as follows

$$\ln\left(\frac{C_0}{C_t}-1\right)=\frac{k_{Th}q_0w}{v}-k_{Th}C_0t$$

Where, k_{Th} (mL/min.mg) is the Thomas rate constant, q_0 (mg/g) is maximum solid-phase concentration, C_0 (mg/L) is the influent Cu ion concentration, C_t (mg/L) is the effluent concentration at time t, w (g) the mass of adsorbent and v (mL min^{-1}) the flow rate. The value of C_t/C_0 is the ratio of outlet and influent Cu ion concentrations. A linear plot of ln $[(C_0/C_t)-1]$ against time (t) was employed (Figure 9a-9c) to determine values of q_0 and k_{Th} from the intercept and slope of the plot.

The column data were fitted to the Thomas model to determine the Thomas rate constant (k_{Th}) and maximum solid-phase concentration (q_0). Results for various operating conditions are listed in Table 2. From Table 2, it is seen that values of determined coefficients (R^2) ranges from 0.92 to 0.955. As the influent concentration increases, value of q_0 increases but value of k_{Th} decreases. The reason is that the driving force for adsorption is the concentration difference between the copper ion on the adsorbent and the copper ion in the solution. With increasing pH, the values of q_0 increases and value of k_{Th} decreases.

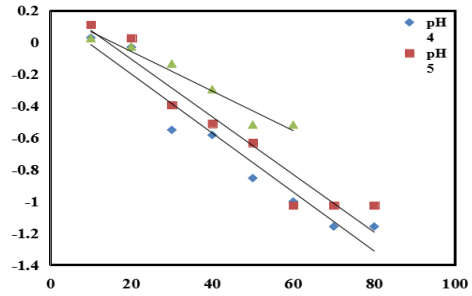

Fig. 9a. Linear Plot of Thomas model with experimental data at different pH, C_0= 600 mg/L, Q_0= 1 mL/min.

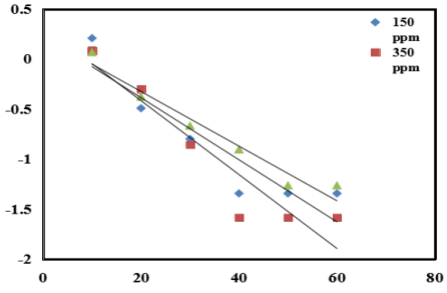

Fig.9b. Linear Plot of Thomas model with experimental data at different concentrations, pH=6, Q_0= 1 mL/min

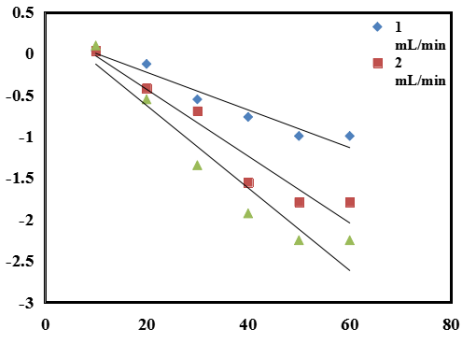

Fig. 9c. Linear Plot of Thomas model with experimental data at different flow rates, C_0= 550 mg/L, pH= 6

Table 2
Thomas model parameters for Cu (II) adsorption at various operating conditions

pH	Q_0 (mL/ min)	C_0 (mg /L)	q_0 (mg/g)	k_{Th} (mL min^{-1}/g)	R^2
4	1	600	5.7	0.034	0.937
5	1	600	8.567	0.030	0.933
6	1	600	9.55	0.020	0.950
6	1	150	1.61	0.26	0.924
6	1	350	3.57	0.125	0.947
6	1	550	4.489	0.049	0.955
6	1	550	5.675	0.04	0.942
6	2	550	10.65 7	0.07	0.931
6	3	550	13.8	0.08	0.925

Adams-Bohart Model

The Adams-Bohart model [41] is used to estimate characteristic parameters such as maximum adsorption capacity (N_0) and kinetic constant (k_{AB}) using a quasi chemical kinetic rate expression. The expression is as follows

$$\ln \frac{C_t}{C_0} = k_{AB} C_0 t - k_{AB} N_0 \frac{Z}{F}$$

Where, C_0 and C_t (mg/L) are the influent and effluent concentration. k_{AB} (mL/mg .min) is the kinetic constant, F (cm/min) is the linear velocity calculated by dividing the flow rate by the column section area, Z (cm) is the bed depth of column and N_0 (mg/L) is maximum ion adsorption capacity per unit volume of adsorbent column. The values of N_0 and k_{AB} can be obtained from the intercept and slope of the linear plot of ln (C_t /C_0) against time (t) as shown in (Figure 10a-10c). Results for various operating conditions are listed in Table 3. From Table 3, as the influent concentration and pH increases, value of N_0 increases but k_{AB} decreases, showing that overall system kinetics was dominated by external mass transfer [42]. However with increasing flow rates, N_0 and k_{AB} increases. The correlation coefficient, R^2 values were between 0.82 and 0.95.

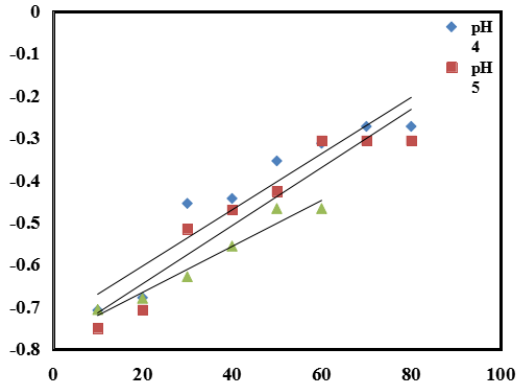

Fig. 10a. Linear Plot of Adams-Bohart model with experimental data at different pH, C_0= 600 mg/L, Q_0= 1 mL/min.

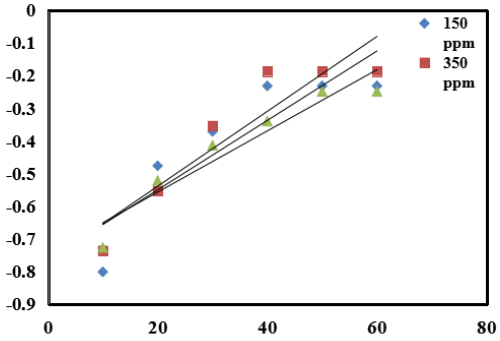

Fig. 10b. Linear Plot of Adams-Bohart model with experimental data at different concentrations, pH=6, Q_0= 1 mL/min.

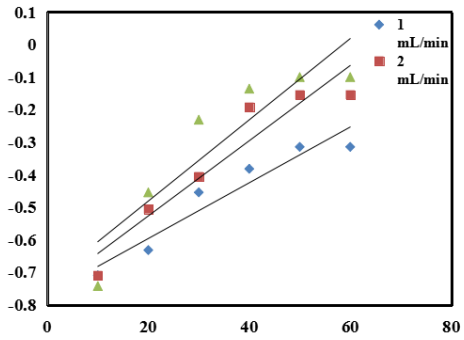

Fig. 17. Linear Plot of Adams-Bohart model with experimental data at different flow rates, C_0= 550 mg/L, pH= 6.

Table 3
Adams-Bohart model parameters for Cu (II) adsorption at various operating conditions

pH	Q_0 (mL/ min)	C_0 (mg/ L)	N_0 (mg/ L)	k_{AB} (mL min^{-1}/mg)	R^2
4	1	600	23.35	0.011	0.893
5	1	600	27.32	0.010	0.908
6	1	600	33.80	0.008	0.957
6	1	150	3.40	0.086	0.863
6	1	350	7.35	0.040	0.935
6	1	550	16.20	0.016	0.908
6	1	550	18.40	0.0145	0.918
6	2	550	26.40	0.020	0.905
6	3	550	34.82	0.0218	0.824

IV. CONCLUSIONS

Magnetite nanoparticles were synthesized by simple and convenient microwave assisted sol-gel method. Microwave results in high reaction temperature which plays an important role in formation and growth of nanoparticles. Thus formation of cubic spinel structured Fe_3O_4 was confirmed by XRD pattern. Microwave heating also results in less reaction time and formation of high crystalline nanoparticles. Thus these microwave synthesized magnetite nanoparticles were used as an adsorbent for Cu (II) ion removal from aqueous solutions using fixed bed adsorption column. Maximum removal efficiency was obtained at pH 6, Cu ion concentration 550 mg/L and flow rate 1 mL/min.

Comparison of Yoon-Nelson, Thomas and Adams-Bohart kinetic models with experimental data was performed and model parameters were determined by analysis for Cu (II) adsorption under various operating conditions. Result showed that the rate constant k_{YN} decreases and the 50% breakthrough time τ increases with increasing pH. With increasing flow rate, the values of τ decreases while the values of k_{YN} increases according to Yoon-Nelson model. Also with increasing initial concentration of copper, q_0 of the adsorbent increases and kinetic constant k_{TH} of model decreases respectively according to Thomas model. Also as influent concentration and pH increases, value of N_0 increases but k_{AB} decreases. Values of R^2 for Adams-Bohart model were found to be lower than that for Thomas and Yoon-Nelson models, thus experimental data fitted well with Thomas and Yoon-Nelson models.

REFERENCES

[1] Environmental Protection Agency, US Environmental protection agency report DC, PA Washington, EPA100/B- 07/001 (2007) 1-13.
[2] L. Jarup, Hazards of heavy metal contamination, Br. Med. Bull. 68 (2003) 167-182.
[3] A. K. Shrivastava, A review on copper pollution and its removal from water bodies by pollution control technologies, Indian J. Environ. Protection 29 (2009) 552-560.
[4] W. Plazinski, W. Rudzinski, Modeling the effect of surface heterogeneity in Equilibrium of heavy metal ion biosorption by using the ion exchange model, Environ. Sci. Technol. 43 (2009) 7465-7471.
[5] M.A. Hasan, Y.T. Selim, K.M. Mohamed, Removal of chromium from aqueous waste solution using liquid emulsion membrane, J. Hazard. Mater. 168 (2009) 1537-1541.
[6] N. K. Srivastava, C.B. Majumder, Novel biofiltration methods for the treatment of heavy metal ions from industrial waste water, J. Hazard. Mater. 151 (2008) 1-8.
[7] B. Yu, Y. Zhang, A. Shukla, S.S. Shukla, K.L. Dorris, The removal of heavy metal

from aqueous solutions by sawdust adsorption-removal of copper, J. Hazard. Mater. 80 (2000) 33-42.

[8] U.K. Garg, M.P. Kaur, V.K. Garg, D. Sud, Removal of hexavalent chromium from aqueous solution by agricultural waste biomass, J. Hazard. Mater. 140 (2007) 60-68.

[9] K. R. Aswin Sidhaarth, J. Jeyanthi, N. Suryanarayan, Comparative studies of removal of lead and zinc from industrial waste water and aqueous solution by iron oxide nanoparticles, performance and mechanism, European J. Sci. Res. 70 (2012) 169-184.

[10]R. Dastjerdi, M. Montazer, A review on the application of inorganic nano-structured materials in the modification of textiles: focus on anti-microbial properties, Colloid Surf B. 279 (2010) 5-18.

[11]L. Zhang, T. Huang, M. Zhang, X. Guo, Z.Yuan, Studies on the capability and behavior of adsorption of thallium on nano-Al_2O_3, J. Hazard. Mater. 157 (2008) 352-357.

[12]S. Sun, H. Zeng, Size-controlled synthesis of magnetite nanoparticles, J. Am. Chem. Soc. 124 (2002) 8204-8205.

[13]S. Si, A. Kotal, T. Mandal, S. Giri, H. Nakamura, T. Kohara, Size-controlled synthesis of magnetite nanoparticles in the presence of polyelectrolytes, Chem. Mater. 16 (2004) 3489-3496.

[14]S. Wan, J. Huang, H. Yan, K. Liu, Size-controlled preparation of magnetite nanoparticles in the presence of graft copolymers, J. Mater. Chem. 16 (2006) 298-303.

[15]N. Neyaz, W.A.Siddiqui, K.K.Nair, Application of surface functionalized iron oxide nanomaterials as a nanosorbents in extraction of toxic heavy metals from ground water: A review, Int. J. Environ. Sci. 4 (2013) 472-483.

[16] S. Hamda, Afnidar, Erdawati, Removal of ion cadmium (II) from water onto chitosan magnetite nanocomposite (CMNs) in fixed beds, in: Proceedings 3rd International Conference on Mathematics and Natural Sciences, Bandung, 2010, p.672.

[17]Q. Yuan, N. Li, Y. Chi, Effect of large pore size of multifunctional mesoporous microsphere on removal of heavy metal ions, J. Hazard. Mater. 255 (2013) 157-165.

[18]J. Wang, S. Zheng, Y. Shao, J. Liu, Z. Xu, D. Zhu, Amino-functionalized Fe_3O_4@SiO_2 core-shell magnetic nanomaterial as a novel adsorbent for aqueous heavy metals removal, J. Colloid Interface Sci. 349 (2010) 293-299.

[19]J. Liu, Z. Zhao, G. Jiang, Coating Fe_3O_4 magnetic nanoparticles with humic acid for high efficient removal of heavy metals in water, Environ. Sci. Technol. 42 (2008) 6949-6954.

[20] X. Xin, Q. Wei, J. Yang, Highly efficient removal of heavy metal ions by amine-functionalized mesoporous Fe_3O_4 nanoparticles, Chem. Eng. J. 184 (2012) 132-140.

[21] M. Shishehbore, A. Afkhami, H. Bagheri, Salicylic acid functionalized silica-coated magnetite nanoparticles for solid phase extraction and preconcentration of some heavy metal ions from various real samples, Chem. Cent. J. (2011) 1-10.

[22]M. Adelia, Y. Yamini, M. Faraji, Removal of copper, nickel and zinc by sodium dodecyl sulphate coated magnetite nanoparticles from water and wastewater samples, Arabian J. Chem. (2012) 1-6.

[23]E.J. Kim, C.S. Lee, Y.Y. Chang, Y.S. Chang, Hierarchically structured manganese oxide coated magnetic nanocomposites for the efficient removal of heavy metal ions from aqueous systems, ACS Appl. Mater. Interfaces 19 (2013) 9628-9634.

[24]F. Zhang, J. Lan, Z. Zhao, Y. Yang, R. Tan, W. Song, Removal of heavy metal ions from aqueous solution using Fe_3O_4–SiO_2-poly (1, 2-diaminobenzene) core-shell sub-micron particles, J. Colloid Interface Sci. 387 (2012) 205-212.

[25]D. Xiao, H. Li, Adsorption performance of carboxylated multi-wall carbon nanotube-Fe_3O_4 magnetic hybrids for Cu(II) in water, New Carbon Mater. 29 (2014) 15-25.

[26]D. Cun ku, L. Xin, Fe_3O_4 nanoparticles decorated multi-walled carbon nanotubes and their sorption properties, Chem. Res. 25 (2009) 936-940.

[27]S. S. Banerjee, D.H. Chen, Fast removal of copper ions by gum arabic modified

magnetic nano-adsorbent, J. Hazard. Mater. 147 (2007) 792-799.

[28]Y. C. Chang, D.H. Chen, Preparation and adsorption properties of monodisperse chitosan-bound Fe_3O_4 magnetic nanoparticles for removal of Cu(II) ions, J. Colloid Interface Sci. 283 (2005) 446-451.

[29]A.Z.M. Badruddoza, A.S.H. Tay, P.Y. Tan, K. Hidajat, M.S. Uddin, Carboxymethyl-β-cyclodextrin conjugated magnetic nanoparticles as nano-adsorbents for removal of copper ions: synthesis and adsorption studies, J. Hazard. Mater. 185 (2011) 1177-1186.

[30]M. Mohaptra, S. Anand, Synthesis and application of nano-structured iron oxide/ hydroxides- a review, Int. J. Eng. Sci. Tech. 2 (2010) 127-146.

[31]D. K. Kim, Y. Zhang, K. Rao, Synthesis and characterization of surfactant coated supermagnetism monodispersed iron oxide nanoparticles, J. Magn. Magn. 225 (2001) 30-36.

[32]S. Shi, J. Hwang, Microwave assisted wet chemical synthesis, advantages, significance, and step to industrialization, J. Mine. Mater. Charct. Engg. 2 (2003) 101-110.

[33] W. Wang, Y. Zhu, M. Raun, Microwave-assisted synthesis and magnetic property of magnetite and hematite nanoparticles, J. Nanoparticle Research 9 (2007) 419-426.

[34]S. Laurent, D. Forge, M. Port, A. Roch, Magnetic iron oxide nanoparticles: synthesis, stabilization, vectorization, physicochemical characterizations and biological applications, Chem Rev. 108 (2008) 2064-2110.

[35]L. Vayssieres, On the effect of nanoparticle size on water-oxide interfacial chemistry. J Phys Chem. 113 (2009) 4733-4736.

[36]A. Hasanpour, M. Niyaifar, M. Asan, Synthesis and characterization of Fe_3O_4 & ZnO nanocomposites by sol-gel method, in: Proceedings 4th International Conference on Nanostructures, Kish Island, 2012, pp.205.

[37]H. Cui, Y. Liu, W. Ren, Structure switch between α- Fe_2O_3, γ- Fe_2O_3 and Fe_3O_4 during large scale and low temperature sol-gel synthesis of nearly monodispersed iron oxide nanoparticles, Adv. Powd. Tech. 24 (2013) 93-97.

[38]P. Yuan, M. Fan, D. Yang, Montmorillonite-supported magnetite nanoparticles for the removal of hexavalent chromium [Cr (VI)] from aqueous solutions, J. Hazard. Mater. 166 (2009) 821-829.

[39] Y. Yoon, J. Nelson, Application of gas adsorption kinetics, Part 1: A theoretical model for respirator cartridge service time, Am. Ind. Hyg. Assoc. J. 45 (1984) 509-516.

[40]H. Thomas, Heterogeneous ion exchange in a flowing system, J. Am. Chem. Soc. 66 (1944) 1466-1664.

[41]G. Bohart, E. Adams, Behavior of charcoal towards chlorine, J.Am. Chem. Soc. 42 (1920) 523-529.

[42]A. Ahmad, B. Hameed, Fixed-bed adsorption of reactive azo dye onto granular activated carbon prepared from waste, J. Hazard. Mater. 175 (2010) 298–303.